



Title	Redox Engineering of Myoglobin by Cofactor Substitution to Enhance Cyclopropanation Reactivity
Author(s)	Kagawa, Yoshiyuki; Oohora, Koji; Himiyama, Tomoki et al.
Citation	Angewandte Chemie – International Edition. 2024, 63(36), p. e202403485
Version Type	VoR
URL	https://hdl.handle.net/11094/97611
rights	This article is licensed under a Creative Commons Attribution-NonCommercial 4.0 International License.
Note	

The University of Osaka Institutional Knowledge Archive : OUKA

<https://ir.library.osaka-u.ac.jp/>

The University of Osaka

Artificial Metalloenzymes

Redox Engineering of Myoglobin by Cofactor Substitution to Enhance Cyclopropanation Reactivity

Yoshiyuki Kagawa, Koji Oohora,* Tomoki Himiyama, Akihiro Suzuki, and Takashi Hayashi*

Abstract: Design of metal cofactor ligands is essential for controlling the reactivity of metalloenzymes. We investigated a carbene transfer reaction catalyzed by myoglobins containing iron porphyrin cofactors with one and two trifluoromethyl groups at peripheral sites (FePorCF₃ and FePor(CF₃)₂, respectively), native heme and iron porphycene (FePc). These four myoglobins show a wide range of Fe(II)/Fe(III) redox potentials in the protein of +147 mV, +87 mV, +42 mV and −198 mV vs. NHE, respectively. Myoglobin reconstituted with FePor(CF₃)₂ has a more positive potential, which enhances the reactivity of a carbene intermediate with alkenes, and demonstrates superior cyclopropanation of inert alkenes, such as aliphatic and internal alkenes. In contrast, engineered myoglobin reconstituted with FePc has a more negative redox potential, which accelerates the formation of the intermediate, but has low reactivity for inert alkenes. Mechanistic studies indicate that myoglobin with FePor(CF₃)₂ generates an undetectable active intermediate with a radical character. In contrast, this reaction catalyzed by myoglobin with FePc includes a detectable iron–carbene species with electrophilic character. This finding highlights the importance of redox-focused design of the iron porphyrinoid cofactor in hemoproteins to tune the reactivity of the carbene transfer reaction.

Introduction

Heme, a porphyrin iron complex, is a ubiquitous cofactor which provides proteins with functions such as diatomic gas-binding, electron transfer, chemical catalysis, and transcriptional regulation among others. The unique reactivity of heme has been investigated in various heme-dependent enzymes. Furthermore, engineered hemoproteins are known to be useful as new catalysts in several reactions including oxidation^[1,2] and reduction,^[3–6] as well as abiological reac-

tions such as carbene transfer,^[7–17] nitrene transfer^[18–20] and radical cyclization.^[21,22] In addition, a protein which does not normally possess a heme cofactor can be converted into an artificial hemoenzyme by creating an artificial heme-binding site in the protein matrix.^[23–29] The reactivities and selectivities of most of these catalysts have been increased by protein engineering through site-directed and site-saturation mutagenesis, high-throughput screening of random mutants and mutation with noncanonical amino acids. On the other hand, replacing heme with an artificial cofactor is another powerful strategy for obtaining highly active artificial metalloenzymes. A porphyrinoid cofactor with iron in the heme center replaced with other metals provides a dramatic change in the reactivity and enhanced catalytic activity for carbene and nitrene transfer reactions.^[30–35] In addition to the metal-substituted cofactors, artificially created metal porphyrinoids have been found to exhibit unique physicochemical properties and reactivities in hemoprotein matrices.^[36–45] Our group has reported a series of hemoproteins reconstituted with metal complexes of porphycene, a constitutional isomer of porphyrin, to produce artificial peroxidase,^[37,38] monooxygenase^[39,40] and cyclopropanase activities.^[41] These proteins are found to exhibit catalytic activity as well as provide detectable active intermediates such as a high-valent metal oxo-species and a metal carbenoid species.

Alkene cyclopropanation by metal-mediated carbene transfer is one of the most studied abiological reactions catalyzed by hemoproteins^[7,8,32,41,46–49] because of the importance of cyclopropane ring in several natural products and bioactive compounds. Although artificial cyclopropanases based on hemoproteins have been reported to catalyze cyclopropanation of styrene derivatives with excellent dia-

[*] Dr. Y. Kagawa, Dr. K. Oohora, Prof. Dr. T. Hayashi
Department of Applied Chemistry,
Graduate School of Engineering, Osaka University,
Suita, Osaka, 565-0871 (Japan)
E-mail: oohora@chem.eng.osaka-u.ac.jp
thayashi@chem.eng.osaka-u.ac.jp

Dr. K. Oohora
Innovative Catalysis Science Division, Institute for Open and
Transdisciplinary Research Initiatives (ICS-OTRI), Osaka University,
Suita, Osaka, 565-0871 (Japan)

Dr. T. Himiyama
Biomedical Research Institute, National Institute of Advanced
Industrial Science and Technology,
Ikeda, Osaka, 563-8577 (Japan)

Dr. A. Suzuki
National Institute of Technology, Ibaraki College,
Hitachinaka, Ibaraki, 312-8508 (Japan)

© 2024 The Author(s). Angewandte Chemie International Edition published by Wiley-VCH GmbH. This is an open access article under the terms of the Creative Commons Attribution Non-Commercial License, which permits use, distribution and reproduction in any medium, provided the original work is properly cited and is not used for commercial purposes.

stereo- and enantioselectivity,^[7,8,16,41,44,46,48,50–53] catalytic activity toward cyclopropanation of inert alkenes remains limited.^[32,54,55] Thus, to achieve cyclopropanation of inert alkenes, an appropriate strategy to enhance the reactivity of the key active intermediate in the catalysis is an important requirement. The metal carbenoid species, which is formed by the reaction of hemoproteins with diazo compounds, is expected to be an active intermediate in the cyclopropanation reaction. It was recently discovered that a porphyrin iron complex in a hemoprotein with a more positive redox potential has higher reactivity for the cyclopropanation reaction. Hilvert and co-workers have reported that a myoglobin (Mb) variant with a noncanonical amino acid possessing an N-methylimidazole moiety as an axial ligand efficiently catalyzes cyclopropanation of styrene.^[15,16] Furthermore, the theoretical studies of Fasan and co-workers suggest that an electron-deficient iron porphyrin can increase the reactivity of carbene intermediates.^[56] This group has also experimentally demonstrated that the combination of Mb variants with the N-methylimidazole axial ligand and an electron-deficient heme analog, diacetyldeuteroheme, which has two electron-withdrawing acetyl substituents at the peripheral positions of the porphyrin framework, exhibits excellent reactivity towards electron-deficient alkenes.^[45] It was recently found that *Amphitrite ornata* dehaloperoxidase variants, which have high redox potential, catalyze the cyclopropanation of electron-deficient vinyl esters.^[57] In this context, we have focused on the use of 13,17-bis(2-carboxyethoxy)-3,8-diethyl-2,12,18-trimethyl-7-trifluoromethylporphyrinatoiron(III) (FePorCF₃) and 13,17-bis(carboxylethyl)-3,7-diethyl-12,18-dimethyl-2,8-ditrifluoromethylporphyrinatoiron(III) (FePor(CF₃)₂),^[58,59] as potent artificial cofactors for Mb with the objective of promoting efficient cyclopropanation. These cofactors contain one or two strong electron withdrawing CF₃ substituents at the β positions to obtain a more positive redox potential, making it suitable for binding to an apo-form of Mb (Figure 1a).^[60]

We have recently reported that myoglobin reconstituted with iron porphycene, 2,7-diethyl-3,6,12,17-tetramethyl-13,16-bis(carboxyethyl)porphycenatoiron(III) (FePc), pro-

motes styrene cyclopropanation with a significantly higher k_{cat} value in Mb and with detection of a carbenoid species.^[41] In this work, four different Mbs with different redox potentials are investigated and compared: native horse heart Mb (nMb), Mb reconstituted with FePor(CF₃)₂ (rMb(FePor(CF₃)₂)), Mb reconstituted with FePorCF₃ (rMb(FePorCF₃)) and Mb reconstituted with FePc (rMb(FePc)). The relationship between the redox potentials of the cofactors in engineered Mbs and the catalytic activities for the cyclopropanation is investigated, and remarkable reactivity of Mb reconstituted with FePor(CF₃)₂ is observed.

Results and Discussion

Characterization of rMb(FePor(CF₃)₂)

Reconstitution of Mb with FePor(CF₃)₂ was conducted by inserting FePor(CF₃)₂ into the apo-form of horse heart Mb (apoMb) which was prepared by removal of native heme (Figure 1b). The reconstituted protein rMb(FePor(CF₃)₂) was characterized by UV/Vis spectroscopy and ESI-MS. The UV/Vis spectrum shows a Soret band with a peak top at 404 nm and broad peaks in the Q-band region (Figure S1), which are generally consistent with the spectrum of previously reported sperm whale Mb (swMb) reconstituted with FePor(CF₃)₂.^[60] In the mass spectrum, multiple ionization peaks attributed to the mass number of rMb(FePor(CF₃)₂) were observed (representative m/z , found: 1766.122, calculated: 1766.119 ($z = +10$), Figure S2).

The crystal structure of the met-form of rMb(FePor(CF₃)₂) was obtained at 1.7 Å resolution by X-ray crystallography (Figure 2). The electron density of FePor(CF₃)₂ was clearly observed in the inherent heme pocket and the iron center of FePor(CF₃)₂ was found to be coordinated by a histidine residue and an H₂O molecule or an OH[−] ion (Figure 2a).^[60] Figure 2b shows the superimposed structure of rMb(FePor(CF₃)₂) with wild-type recombinant horse heart Mb (wtMb). The root-mean-square deviation (RMSD) for all Ca atoms is only 0.222 Å. The structure in the vicinity of the cofactor and overall protein structure are identical to those of wtMb. The bond lengths from the Fe to the Nε2-

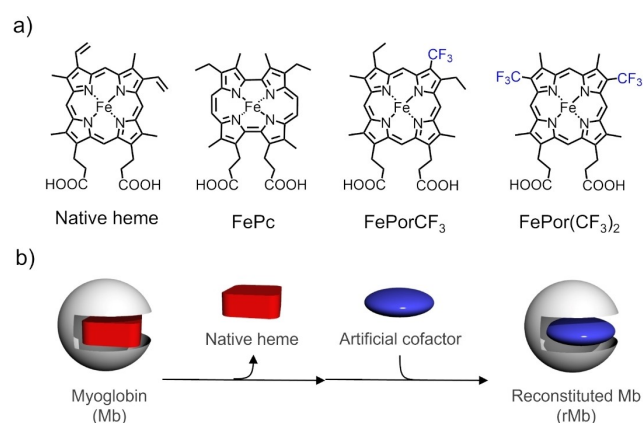


Figure 1. a) Chemical structures of heme and artificial cofactors. b) Reconstitution of Mb with an artificial cofactor.

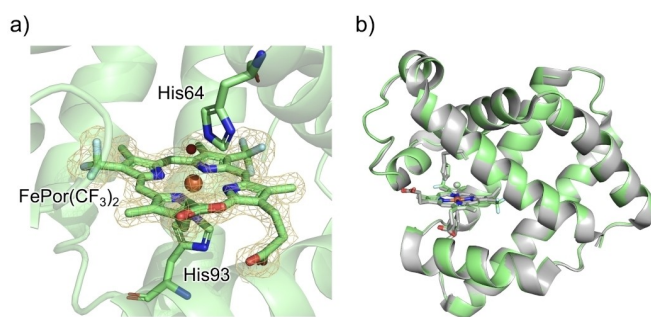


Figure 2. Crystal structure of rMb(FePor(CF₃)₂). a) The heme pocket with the 2F_o-F_c electron density (1.0 σ contours) of the FePor(CF₃)₂ molecule. b) Superimposed structure of rMb(FePor(CF₃)₂) (green) and wild-type horse heart Mb (gray, PDB: 1WLA).

atom of the histidine residue and the Fe to the oxygen atom of the H₂O molecule or the OH[−] ion are 2.1 Å and 2.2 Å, respectively. These lengths are the same as those of wtMb. The orientations of two propionate side chains are similar to those of wtMb. The hydrogen bonding network including the propionate side chains is also maintained. The structure of the reconstituted Mb is also similar to the reconstituted sperm whale Mb with FePorCF₃ (rswMb(FePorCF₃))^[60] (Figure S3). In the rMb(FePor(CF₃)₂), a single cofactor structure was observed because of its symmetric nature. In contrast, FePorCF₃ in Mb displays two orientations derived from its asymmetric structure. This is the first X-ray crystal structure of Mb containing FePor(CF₃)₂.

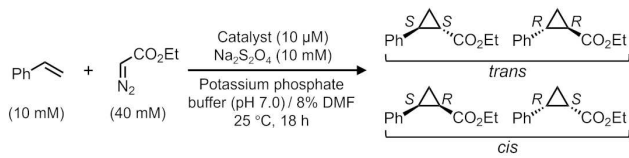
To elucidate the role of the CF₃ substituents in the electronic property, we conducted spectroelectrochemical measurements. Absorption spectral changes of rMb(FePorCF₃) and rMb(FePor(CF₃)₂) measured at applied potentials include several clear isosbestic points (Figure S4). The Fe^{II}/Fe^{III} redox potentials of rMb(FePorCF₃) and rMb(FePor(CF₃)₂) in 100 mM potassium phosphate buffer at pH 7.0 were determined to be 87 ± 3 mV and 147 ± 3 mV vs. NHE, respectively (Figure S5 and S6). The value of rMb(FePor(CF₃)₂) is positively shifted by 102 mV and 345 mV relative to that of nMb (45 mV vs NHE)^[61] and rMb(FePc) (−198 mV vs NHE)^[36] respectively. As expected, the effect of two CF₃ substituents to the positive shift of the redox potentials is larger than the effect induced by one CF₃ substituent. Notably, the effect of the two CF₃ substituents is greater than that of the two acetyl substituents at 3- and 8-positions, where the Fe^{II}/Fe^{III} redox potential is positively shifted by only 20 mV relative to the protein containing native heme.^[45] Thus, the CF₃ substituent in the β position of the porphyrin framework is expected to significantly enhance the reactivity of the carbene intermediate.

Styrene Cyclopropanation

Using the cofactors and Mbs with different redox potentials as catalysts, we investigated styrene cyclopropanation with ethyl diazoacetate (EDA) as a carbene source in the presence of dithionite under a N₂ atmosphere (Table 1). First, the reactions catalyzed by bare cofactors (without a protein matrix) were evaluated. FePor(CF₃)₂ which has the more positive redox potential exhibits a high TON value of 575 for the cyclopropanation reaction compared with native heme (TON=150), FePc (TON=47) and FePorCF₃ (TON=158). Enhancement of the reaction yield by an electron deficient porphyrinoid ligand is also observed in iron tetraphenylporphyrin-based catalysts.^[62] Next, styrene cyclopropanation was performed in a catalytic system using a mixed solution of FePor(CF₃)₂ or FePorCF₃ and apoMb at a molar ratio of 1:2 in the reaction solution. The in situ prepared reconstituted Mbs, hereafter designated rMb*(FePor(CF₃)₂) and rMb*(FePorCF₃), respectively. rMb*(FePor(CF₃)₂) was found to catalyze the reaction more efficiently than nMb, rMb(FePc) and rMb*(FePorCF₃) and the TON is clearly enhanced due to the suppression of the EDA dimerization with higher diastereo- and enantioselectivity relative to the corresponding bare cofactor. The effect of the presence of the protein matrix on the TON of FePor(CF₃)₂ is more apparent at low concentrations of EDA: The TON of rMb*(FePor(CF₃)₂) is increased by 5.6-fold compared to the TON of FePor(CF₃)₂ (Table S1). These findings and crystal structure data suggest that the difference in the reactivity between rMb(FePor(CF₃)₂) and nMb is due to the CF₃ substitution and not to any structural perturbations occurring upon reconstitution.

Although diastereomeric excess (*de*) values obtained by rMb*(FePor(CF₃)₂) were found to be moderate, the enantiomeric excess (*ee*) values were limited to 4% and 16% for

Table 1: Evaluation of styrene cyclopropanation with 4 eq. of EDA.^[a]

					
Entry	Catalyst	TON	<i>de</i> ^[c]	<i>ee</i> ^[d]	<i>ee</i> ^[e]
1 ^[b]	Hemin	150 ± 3	83 ± 0%	4 ± 1%	0 ± 0%
2	FePc	47 ± 4	64 ± 0%	0 ± 1%	0 ± 1%
3 ^[b]	FePorCF ₃	158 ± 16	85 ± 0%	0 ± 0%	0 ± 0%
4 ^[b]	FePor(CF ₃) ₂	575 ± 37	84 ± 0%	8 ± 0%	1 ± 1%
5	Mb	433 ± 11	86 ± 1%	6 ± 1%	−3 ± 1%
6	rMb(FePc)	302 ± 43	99 ± 0%	20 ± 10%	96 ± 2%
7 ^[b]	rMb*(FePorCF ₃)	602 ± 87	86 ± 1%	2 ± 2%	1 ± 0%
8 ^[b]	rMb*(FePor(CF ₃) ₂)	710 ± 16	88 ± 2%	16 ± 2%	−4 ± 2%
9	swMb ^{H64V/V68A}	510 ± 64	98 ± 1%	83 ± 8%	99 ± 0%
10 ^[b]	rswMb ^{H64V/V68A} *(FePor(CF ₃) ₂)	810 ± 34	98 ± 1%	−53 ± 10%	99 ± 1%

[a] Conditions: [catalyst] = 10 μM or [cofactor] = 10 μM and [apoMb] = 20 μM, [styrene] = 10 mM, [EDA] = 40 mM, [Na₂S₂O₄] = 10 mM in 100 mM potassium phosphate buffer (pH 7.0) containing 8% DMF at 25 °C for 18 h under a N₂ atmosphere. Results are presented as mean ± standard deviation (n ≥ 2). [b] A solution containing 2% DMSO. [c] *de* for the *trans* products. [d] *ee* for (1*S*,2*R*)-cyclopropane in the *cis* products. [e] *ee* for (1*S*,2*S*)-cyclopropane in the *trans* products.

both *trans* and *cis* products, respectively. To improve the enantioselectivity, the apo-form of swMb H64V/V68A variant (swMb^{H64V/V68A}) was used as a protein matrix because the variant is known from a previous study to provide high diastereo- and enantioselectivity values for styrene cyclopropanation.^[8] rswMb^{H64V/V68A}*(FePor(CF₃)₂) where FePor(CF₃)₂ was mixed with the apo-form variant generates the *trans*-(1*S*,2*S*)-cyclopropane product with excellent diastereo- and enantioselectivity (98% *de* and 99% *ee*) with higher TON than that of swMb^{H64V/V68A} (entry 10 of Table 1). The selectivity was expected because FePor(CF₃)₂ is located in a reaction environment similar to the variant containing heme. The findings suggest that FePor(CF₃)₂ with a highly positive redox potential can be utilized for various enantioselective cyclopropanation reactions when combination with an optimized protein matrix.

To evaluate the kinetics of the catalysis, initial turnover frequency (TOF) values were determined for the reaction catalyzed by rMb*(FePor(CF₃)₂) and nMb under conditions of 0.1–2.0 mM styrene and 20 mM EDA. Michaelis–Menten kinetics parameters were determined for both catalysts (Figure 3a). The *k*_{cat} and *K*_M values of rMb*(FePor(CF₃)₂) and nMb are summarized in Table 2, where the values of rMb(FePc) determined in our previous report are also shown.^[41] The rMb(FePc) protein provided the highest *k*_{cat} value, and the lowest TON in the 18 h reaction. The *k*_{cat}

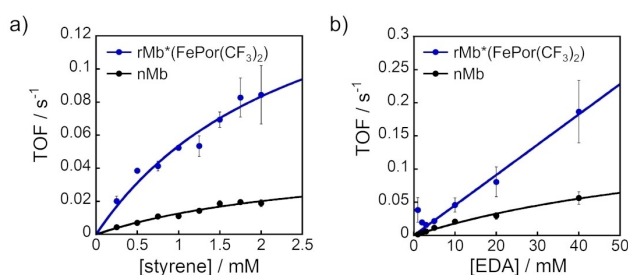


Figure 3. Plots of the TOF of styrene cyclopropanation with EDA. Conditions: [nMb] = 1 μM or [FePor(CF₃)₂] = 1 μM and [apoMb] = 2 μM, [Na₂S₂O₄] = 10 mM in 100 mM potassium phosphate buffer (pH 7.0) containing 8% DMF at 25 °C for 30 min under a N₂ atmosphere. 0.2% DMSO was contained for the reactions catalyzed by rMb*(FePor(CF₃)₂). a) [styrene] = 0.2–2.0 mM, [EDA] = 20 mM; b) [styrene] = 2.0 mM, [EDA] = 1.0–40 mM. Data plotted represent the means with standard deviations (*n* ≥ 2).

Table 2: Michaelis–Menten parameters with various concentrations of styrene.^[a]

Catalyst	<i>k</i> _{cat} (s ^{−1})	<i>K</i> _M (mM)	<i>k</i> _{cat} / <i>K</i> _M (mM s ^{−1})
rMb(FePc) ^[b]	1.7 ± 0.3	1.3 ± 0.4	1.3 ± 0.5
nMb	0.05 ± 0.01	2.9 ± 1.3	0.017 ± 0.008
rMb*(FePor(CF ₃) ₂) ^[c]	0.19 ± 0.05	2.5 ± 1.1	0.078 ± 0.040

[a] Conditions: [nMb] = 1 μM or [FePor(CF₃)₂] = 1 μM and [apoMb] = 2 μM, [styrene] = 0.2–2.0 mM, [EDA] = 20 mM, [Na₂S₂O₄] = 10 mM in 100 mM potassium phosphate buffer (pH 7.0) containing 8% DMF at 25 °C for 30 min under a N₂ atmosphere. Results are presented as mean ± standard deviation (*n* ≥ 2). [b] Reported values.^[41] [c] Containing 0.2% DMSO.

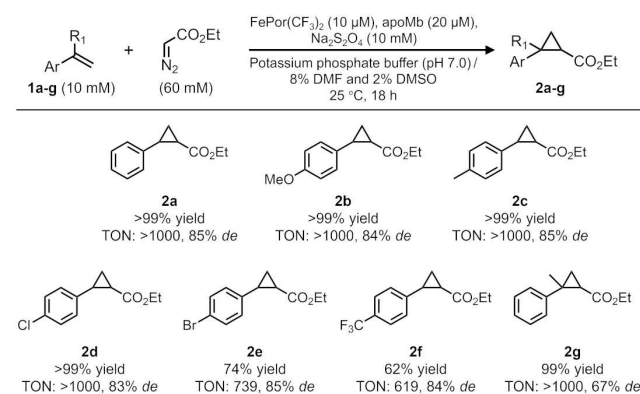
value of rMb*(FePor(CF₃)₂) is almost 4-fold higher than that of nMb. Next, the TOF values measured under conditions with various concentrations of EDA (Figure 3b) suggest that the plots of rMb*(FePor(CF₃)₂) did not reach a plateau even with the high concentration of EDA (Table 3). The *K*_M value of nMb is around 87 mM, while rMb(FePc) shows a saturation curve with a *K*_M value of 1.9 mM. Therefore, the reaction rates for nMb and rMb*(FePor(CF₃)₂) are highly dependent on the EDA concentration. This means that the formation of an active intermediate for rMb*(FePor(CF₃)₂) dominantly limits the rate of the overall reaction. Although a bare cofactor, FePor(CF₃)₂, exhibits similar Michaelis–Menten parameters as rMb*(FePor(CF₃)₂) under conditions of various styrene concentrations and 20 mM EDA, the TOF value evaluated under 40 mM EDA concentration is significantly lower than that of rMb*(FePor(CF₃)₂) (Figure S7). The protein matrix would suppress the reaction of the carbene intermediate with another EDA (a side reaction known as dimerization of EDA) or the inactivation of the cofactor. Thus, the FePor(CF₃)₂ cofactor requires a protein matrix for efficient catalysis with enhanced chemoselectivity.

To explore the scope of substrates for rMb*(FePor(CF₃)₂), the cyclopropanation of substituted styrenes was evaluated using 6 equivalents of EDA (Scheme 1). The

Table 3: Michaelis–Menten parameters with various concentrations of EDA.^[a]

Catalyst	<i>k</i> _{cat} (s ^{−1})	<i>K</i> _M (mM)	<i>k</i> _{cat} / <i>K</i> _M (mM s ^{−1})
rMb(FePc) ^[b]	2.1 ± 0.2	1.9 ± 0.6	1.1 ± 0.4
nMb	0.18 ± 0.05	87 ± 35	0.0021 ± 0.001
rMb*(FePor(CF ₃) ₂) ^[c]	–	–	0.0046 ± 0.0005 ^[d]

[a] Conditions: [nMb] = 1 μM or [FePor(CF₃)₂] = 1 μM and [apoMb] = 2 μM, [styrene] = 2.0 mM, [EDA] = 1–40 mM, [Na₂S₂O₄] = 10 mM in 100 mM potassium phosphate buffer (pH 7.0) containing 8% DMF at 25 °C for 30 min under a N₂ atmosphere. –: not determined. Results are presented as mean ± standard deviation (*n* ≥ 2). [b] Reported values.^[41] [c] Containing 0.2% DMSO. [d] Calculated from the slope of the linear correlation.



Scheme 1. Cyclopropanation of terminal styrene derivatives by rMb*(FePor(CF₃)₂).^[a] [a] Conditions: [FePor(CF₃)₂] = 10 μM and [apoMb] = 20 μM, [styrene] = 10 mM, [EDA] = 60 mM, [Na₂S₂O₄] = 10 mM in 100 mM potassium phosphate buffer (pH 7.0) containing 8% DMF and 2% DMSO at 25 °C for 18 h under a N₂ atmosphere.

catalyst promotes cyclopropanation of styrene (**1a**), *p*-methoxystyrene (**1b**), *p*-methylstyrene (**1c**) and *p*-chlorostyrene (**1d**) with >99 % yield and TON >1000 under these conditions. The electron-deficient alkenes were also converted to the corresponding cyclopropane derivatives with good yields, **1e** (74 %, TON=739) and **1f** (62 %, TON=619). Cyclopropanation of a more sterically hindered substrate, α -methylstyrene (**1g**), was efficiently catalyzed by $\text{rMb}^*(\text{FePor}(\text{CF}_3)_2)$ with excellent yield and TON (>99 %, >1000). The racemic products **2d–2g** were obtained in these reactions because the native protein matrix was used. Comparison of the TON values of the three Mbs for **1g** is similar to that of **1a**: The order of Mbs providing higher TON values is $\text{rMb}(\text{FePc}) < \text{nMb} < \text{rMb}^*(\text{FePor}(\text{CF}_3)_2)$ (Table S2). Thus, $\text{rMb}^*(\text{FePor}(\text{CF}_3)_2)$ was found to efficiently promote the cyclopropanation of terminal styrene derivatives.

Cyclopropanation of β -Methylstyrene, an Internal Alkene

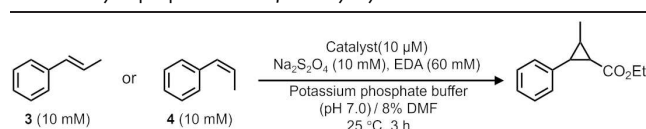
Iron porphyrin-based catalysts usually demonstrate low activity for internal alkenes.^[8,62] We evaluated the reaction with β -methylstyrene as an internal alkene substrate (Table 4). In the case of *trans*- β -methylstyrene (**3**), $\text{rMb}^*(\text{FePor}(\text{CF}_3)_2)$, $\text{rMb}^*(\text{FePorCF}_3)$ and nMb gave two enantiomeric pairs with TON of 6.0, 2.8 and 1.0, respectively. The enantiomeric pairs are assigned to the *trans* configuration with respect to the methyl and phenyl groups in the cyclopropanation product. No product was detected in the reaction with $\text{rMb}(\text{FePc})$. The TOF of $\text{rMb}^*(\text{FePor}(\text{CF}_3)_2)$ (0.2 min⁻¹) is ten times higher than that of nMb (0.02 min⁻¹) (Table S3). $\text{rMb}^*(\text{FePor}(\text{CF}_3)_2)$, $\text{rMb}^*(\text{FePorCF}_3)$ and nMb also catalyze the cyclopropanation of *cis*- β -methylstyrene with TON of 1.6, 0.8 and 0.4, respectively. In this reaction,

these catalysts generate four enantiomeric pairs, including both *cis* and *trans* isomers with respect to the methyl and phenyl groups (Entry 5 and 6 of Table 4) as a result of flipping of the methyl group during the reaction. This result suggests that the reactions catalyzed by nMb and $\text{rMb}^*(\text{FePor}(\text{CF}_3)_2)$ may proceed by a stepwise mechanism (see below), whereas further support by computational simulations will be required to clarify the mechanism. Taken together, these results indicate that $\text{rMb}^*(\text{FePor}(\text{CF}_3)_2)$ provides higher reactivity toward internal alkenes than the other two Mbs.

Cyclopropanation of 1-Octene, an Aliphatic Alkene

The catalytic activity toward the cyclopropanation of an aliphatic alkene was investigated using 1-octene as a substrate. The TON and TOF values of the reaction with each Mb are summarized in Table 5. The reaction catalyzed by $\text{rMb}^*(\text{FePor}(\text{CF}_3)_2)$ was smoothly promoted with TON of 33 in 6 h (Figure 4), and its TON is 165-fold higher than that of nMb (TON=0.2). In the case of $\text{rMb}(\text{FePc})$, no activity was observed. The order of TON values follows the order of the redox potentials: $\text{rMb}^*(\text{FePor}(\text{CF}_3)_2) > \text{rMb}^*(\text{FePorCF}_3) > \text{nMb} > \text{rMb}(\text{FePc})$. In addition, with only the cofactor $\text{FePor}(\text{CF}_3)_2$, the amount of product is lower than that with $\text{rMb}^*(\text{FePor}(\text{CF}_3)_2)$. The TOF value of $\text{rMb}^*(\text{FePor}(\text{CF}_3)_2)$ is 2 min⁻¹, while that of $\text{rMb}^*(\text{FePorCF}_3)$ and nMb are 0.4 min⁻¹ and 0.1 min⁻¹, respectively. Previously, Mb reconstituted with the electron-deficient heme was found to act as an Mb-based catalyst for an inert alkene.^[45] Considering these results, the positive redox potential is a key property that enhances the activity of the catalyst toward the cyclopropanation of inert alkenes. The electron-deficient cofactor should generate active carbene species enough to react with aliphatic alkenes, while the carbene

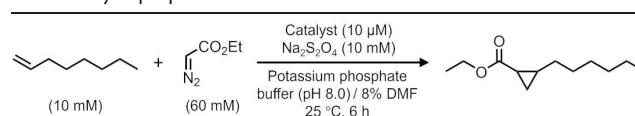
Table 4: Cyclopropanation of β -methylstyrene.^[a]



Entry	Substrate	Catalyst	TON	<i>trans</i> : <i>cis</i> ^[c]
1	3	$\text{rMb}(\text{FePc})$	N.D.	–
2	3	nMb	1.0 ± 0.1	100:0
3 ^[b]	3	$\text{rMb}^*(\text{FePorCF}_3)$	2.8 ± 0.4	100:0
4 ^[b]	3	$\text{rMb}^*(\text{FePor}(\text{CF}_3)_2)$	6.0 ± 0.1	100:0
5	4	$\text{rMb}(\text{FePc})$	N.D.	–
6	4	nMb	0.4 ± 0.0	48:52
7 ^[b]	4	$\text{rMb}^*(\text{FePorCF}_3)$	0.8 ± 0.1	46:54
8 ^[b]	4	$\text{rMb}^*(\text{FePor}(\text{CF}_3)_2)$	1.6 ± 0.1	41:59

[a] Conditions: [catalyst]=10 μM or [cofactor]=10 μM and [apoMb]=20 μM, [β -methylstyrene]=10 mM, [EDA]=60 mM, [$\text{Na}_2\text{S}_2\text{O}_4$]=10 mM in 100 mM potassium phosphate buffer (pH 7.0) containing 8 % DMF at 25 °C for 3 h under a N_2 atmosphere. N.D.: not detected. –: not determined. Results are presented as mean ± standard deviation ($n \geq 2$). [b] Containing 2 % DMSO. [c] Ratio of *trans* and *cis* configurations respect to the methyl and phenyl groups.

Table 5: Cyclopropanation of 1-octene.^[a]



Catalyst	TON	TOF (min ⁻¹) ^[c]	<i>de</i> ^[d]
$\text{rMb}(\text{FePc})$	N.D.	–	–
nMb	0.2 ± 0.1	0.1 ± 0.0	60 ± 8%
$\text{rMb}^*(\text{FePorCF}_3)$	4.5 ± 1.1	0.4 ± 0.1	65 ± 2%
$\text{rMb}^*(\text{FePor}(\text{CF}_3)_2)$ ^[b]	33 ± 5	2.0 ± 0.2	67 ± 3%
$\text{FePor}(\text{CF}_3)_2$ ^[b]	8 ± 2	–	62 ± 0%

[a] Conditions: [catalyst]=10 μM or [cofactor]=10 μM and [apoMb]=20 μM, [1-octene]=10 mM, [EDA]=60 mM, [$\text{Na}_2\text{S}_2\text{O}_4$]=10 mM in 100 mM potassium phosphate buffer (pH 8.0) containing 8 % DMF at 25 °C for 6 h under a N_2 atmosphere. N.D.: not detected. –: not determined. Results are presented as mean ± standard deviation ($n \geq 2$). [b] Containing 2 % DMSO. [c] Conditions: [catalyst]=10 μM or [$\text{FePor}(\text{CF}_3)_2$]=10 μM and [apoMb]=20 μM, [1-octene]=2.0 mM, [EDA]=20 mM, [$\text{Na}_2\text{S}_2\text{O}_4$]=10 mM in 100 mM potassium phosphate buffer (pH 7.0) containing 8 % DMF at 25 °C for 3 min under a N_2 atmosphere. [d] *de* for *trans* product.

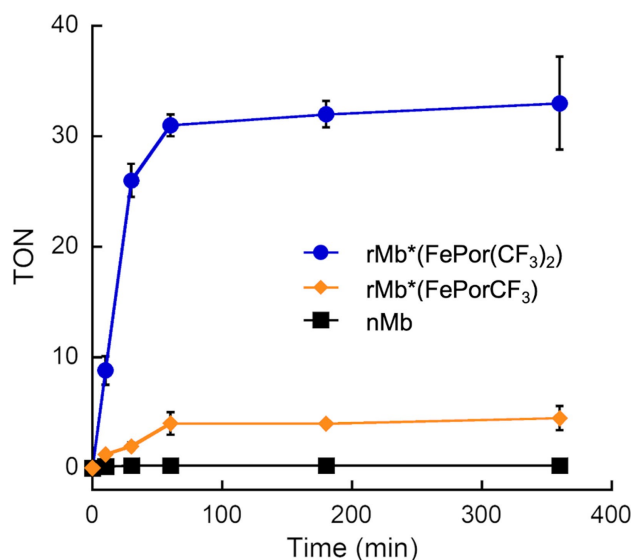


Figure 4. Time course plots of TON for cyclopropanation of 1-octene by nMb, rMb*(FePorCF₃) and rMb*(FePor(CF₃)₂). Data plotted represent the means with standard deviations ($n \geq 2$).

intermediate of rMb(FePc) has insufficient reactivity. We found that the TON value of rMb*(FePor(CF₃)₂) highly depends on the ratio of 1-octene and EDA (Table S4). As a result, using 6 equivalents of EDA against the alkene provides the best condition. Notably, the TON value of 33 by rMb*(FePor(CF₃)₂) is higher than that by Mb^{H93G/H64A/V68F} containing an Ir porphyrin complex (TON=20 by a single addition of 6 eq. EDA).^[63] However, the product is racemic. Further studies using apoMb variants are necessary to achieve enantioselective reaction.

Aerobic Styrene Cyclopropanation

The cyclopropanation reactions catalyzed by rMb*(FePor(CF₃)₂) and nMb without additional reductant were investigated under aerobic and anaerobic conditions (Figure 5). First, since rMb*(FePor(CF₃)₂) has the more positive redox potential and is easily reduced by EDA,^[45,62] we assumed that it catalyzes the reaction under aerobic conditions without any additional reductants. Moreover, since a low affinity of deoxy-rswMb(FePor(CF₃)₂) for dioxygen has been reported,^[60,64] the binding of dioxygen to the reduced cofactor, which would prevent the cyclopropanation, would be suppressed. As expected, rMb*(FePor(CF₃)₂) shows a TON of 774 under anaerobic conditions without additional reductant, which is almost consistent with the TON obtained by the reaction in the presence of dithionite under anaerobic conditions. This catalyst also produces trace amounts of the product under aerobic conditions (TON=4), while nMb gives no product. These findings provide clear evidence that ferric rMb*(FePor(CF₃)₂) can be easily reduced to the ferrous form which is the starting point for the catalysis. Furthermore, rswMb^{H64V/V68A}*(FePor(CF₃)₂) shows a 17 % yield and a TON of 167 with 98 % *de* and 99 % *ee* under

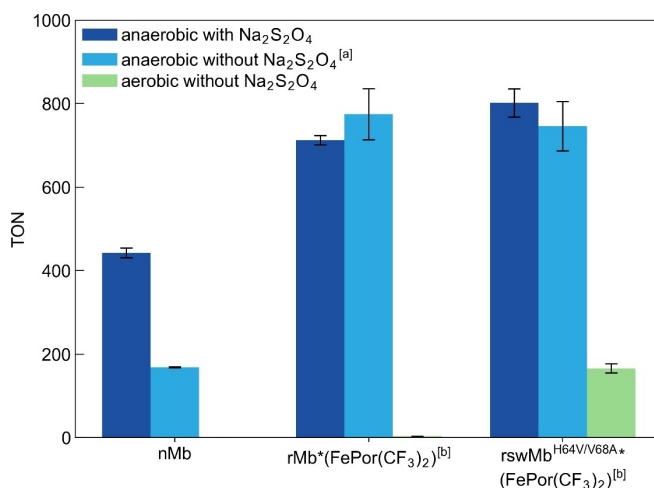


Figure 5. Styrene cyclopropanation with and without dithionite measured under anaerobic and aerobic conditions. Conditions: [catalyst] = 10 μ M or [FePor(CF₃)₂] = 10 μ M and [apoMb] = 20 μ M, [styrene] = 10 mM, [EDA] = 40 mM, [Na₂S₂O₄] = 10 mM in 100 mM potassium phosphate buffer (pH 7.0) containing 8 % DMF at 25 °C for 18 h. a) Containing glucose (25 mM), glucose oxidase (20 unit) and catalase (280 unit). b) Containing 2 % DMSO. Data plotted represent the means with standard deviations ($n \geq 2$).

aerobic conditions without additional reductant. The results indicate that 22 % activity is maintained compared to the reaction in the presence of dithionite under anaerobic conditions. The enhancement of tolerance to dioxygen is caused by mutation of His64, an essential residue for the high dioxygen binding affinity of nMb.^[65] Native heme-containing swMb^{H64A/V68A} is known to generate trace amounts of product without additional reductant under aerobic conditions.^[15,44] Thus, the binding of FePor(CF₃)₂ to the protein matrix synergistically provides dioxygen tolerance to the reaction.

Mechanistic Study

To investigate the reaction mechanism of the cyclopropanation by Mbs, a Hammett analysis was performed based on the relative rate of cyclopropanation of *para*-substituted styrenes against non-substituted styrene in competition experiments (Table S5). First, the $\log(k_X/k_H)$ values for the cyclopropanation of **1a–1d** and **1f** by Mbs were then plotted against the Hammett substituent constants (Figure 6a–c). The linear correlation of the $\log(k_X/k_H)$ of rMb(FePc) for the constants was observed with a negative slope ($R^2=0.90$, $\rho=-0.80$), whereas a moderate correlation in rMb*(FePor(CF₃)₂) ($R^2=0.64$, $\rho=-0.34$) was obtained. In the case of nMb, the fitting analysis of the plots does not yield satisfactory results ($R^2=0.05$, $\rho=0.08$). This finding led us to consider the possibility of a radical mechanism. This is because a previous study has proposed that the electron-deficient heme exhibits radical reactivity.^[44] When the values were plotted against Jiang and Ji's spin-delocalization substituent constants σ^* ,^[66] a good linear correlation was

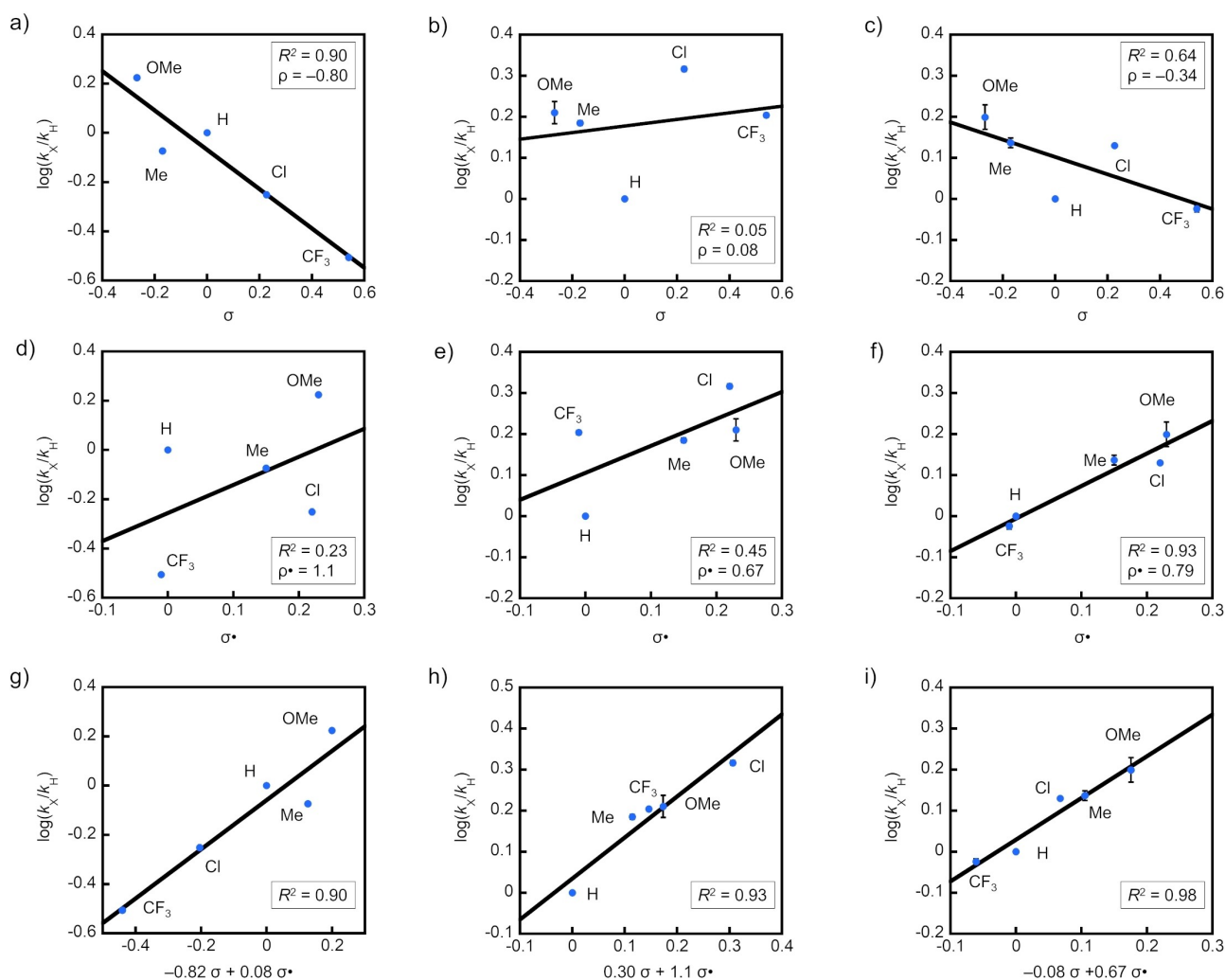


Figure 6. Hammett analysis of cyclopropanation of *para*-substituted styrenes (substituents: –OMe, –Me, –H, –Cl, –CF₃). Top: $\log(k_X/k_H)$ plots against Hammett constants for the cyclopropanation catalyzed by a) rMb(FePc), b) nMb, c) rMb*(FePor(CF₃)₂). Middle: $\log(k_X/k_H)$ plots against Jiang and Ji's spin-delocalization constants for the cyclopropanation catalyzed by d) rMb(FePc), e) nMb, f) rMb*(FePor(CF₃)₂). Bottom: $\log(k_X/k_H)$ plots against Hammett and Jiang and Ji's spin-delocalization constants. g) rMb(FePc), h) nMb, i) rMb*(FePor(CF₃)₂). Conditions: [catalyst] = 1 μ M or [FePor(CF₃)₂] = 1 μ M and [apoMb] = 2 μ M, [styrene] = 0.5 mM, [*para*-substituted styrene] = 0.5 mM, [EDA] = 5.0 mM, [Na₂S₂O₄] = 10 mM in 100 mM potassium phosphate buffer (pH 7.0) containing 8% DMF at 25 °C for 10 min under a N₂ atmosphere. 0.2% DMSO was contained for the reactions catalyzed by rMb*(FePor(CF₃)₂). The reaction catalyzed by rMb(FePc) was quenched in 1 min. Data plotted represent the means with standard deviations ($n \geq 2$).

obtained in the cyclopropanation by rMb*(FePor(CF₃)₂) ($R^2=0.93$, $\rho^*=0.79$) (Figure 6f). For nMb, Jiang and Ji's spin-delocalization substituent constants σ^* show a better correlation with $\log(k_X/k_H)$ values ($R^2=0.45$, $\rho^*=0.67$) than the usual Hammett substituent constants σ (Figure 6e). In contrast, the $\log(k_X/k_H)$ values determined for rMb(FePc) are not correlated with the σ^* constants (Figure 6d). Next, considering both polar effects and radical stabilization effects, the $\log(k_X/k_H)$ values were fitted to a dual-parameter Hammett equation $\log(k_X/k_H)=\rho\sigma+\rho^*\sigma^*$ by multiple regression.^[67] Each instance of catalysis shows a good relationship with this equation, resulting in a R^2 value over 0.9 (Figure 6g–i). The large $|\rho/\rho^*|$ ratio of 12 in rMb(FePc) indicates that the polar effect is dominant in the reaction. nMb and rMb*(FePor(CF₃)₂) show large contributions of

radical stabilization effects: $|\rho/\rho^*|$ ratios are 0.26 and 0.12, respectively. Thus, the Hammett analysis suggests the formation of intermediates with electrophilic character in rMb(FePc) and radical character in nMb and rMb*(FePor(CF₃)₂), respectively. Particularly, the latter finding supports the result of the formation of four enantiomeric pairs in the cyclopropanation of *cis*- β -methylstyrene (see above). Radical spin-trap analysis was performed using 5,5-dimethyl-1-pyrroline *N*-oxide (DMPO) as a spin trap reagent. rMb(FePc) remained about 80% of the TON value in the presence of DMPO compared to the reaction without DMPO, whereas the reaction with rMb(FePor(CF₃)₂) was clearly inhibited by DMPO, resulting in a 70% loss of TON (Table S7). This result also confirms that the intermediate of cyclopropanation by rMb(FePor(CF₃)₂) has a radical charac-

ter. To detect the carbene intermediates of the catalysts, transient absorption spectral changes were monitored using a stopped flow apparatus. When the ferrous states of nMb or rMb*(FePor(CF₃)₂) were mixed with EDA, UV/Vis spectral changes were observed, suggesting the formation of a new species (Figure S8). However, double-mixing stopped flow experiments indicate that the observed species does not further react with styrene. The mass number of the new species corresponds to the value of the carbene adduct of the cofactor (Figure S9). Therefore, the new species might be an unreactive alkylated^[68] or Fe–C–N(pyrrole) bridging carbene adduct.^[16,69] These results indicate that the active intermediates of nMb and rMb*(FePor(CF₃)₂) are undetectable, while the reactive intermediate of the rMb(FePc) has been observed in our previous work.^[41] This is probably because the lifetime of the active intermediates for nMb and rMb*(FePor(CF₃)₂) is too short to detect in stopped flow experiments due to the formation of the unreactive adduct. This result suggests that the active intermediate of rMb(FePc) is relatively stable compared to the active intermediates of nMb and rMb*(FePor(CF₃)₂).

From these results, a plausible mechanism for the reaction catalyzed by rMb*(FePor(CF₃)₂) is proposed and depicted in Scheme 2. In the case of the rMb*(FePor(CF₃)₂), the generated active carbene species has a radical character. The active intermediates react with an alkene substrate by a stepwise radical mechanism to produce the cyclopropanated products. In the case of rMb(FePc), the ferrous state of the cofactor reacts with EDA to generate the relatively stable and electrophilic carbene intermediate which promotes cyclopropanation of alkenes.

Conclusion

In summary, we identified a relationship between the reactivity of alkene cyclopropanation and redox potentials of four myoglobins with different cofactors. The protein containing FePor(CF₃)₂, which has a more positive redox potential, exhibits remarkable reactivity for the cyclopropanation of inert alkenes.

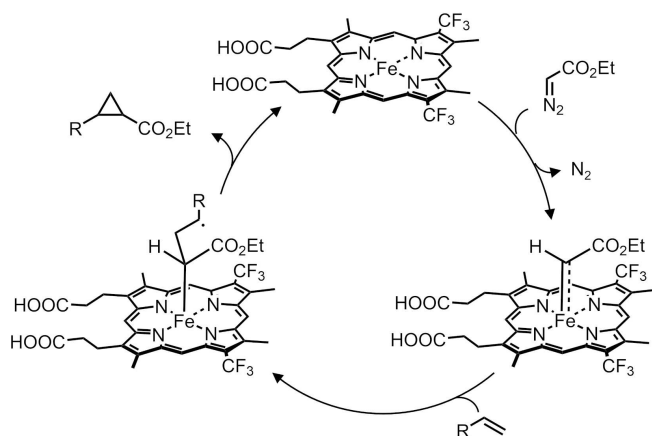
In contrast, the protein reconstituted with FePc, which has a more negative redox potential,^[70] demonstrated decreased reactivity for an inert alkene, while accelerating the formation of the carbene intermediate. The mechanistic studies presented herein suggest that two myoglobins with different cofactors, FePor(CF₃)₂ and FePc, demonstrate different character for cyclopropanation, a radical character and an electrophilic character, respectively. It is interesting that the two results indicate trade-off characteristics in the carbene formation and carbene insertion into alkenes. These results indicate that tuning of the redox potential of the iron center in the heme cofactor serves as a useful strategy for controlling and/or enhancing the cyclopropanation reactivity of myoglobin, a simple dioxygen storage protein. FePor(CF₃)₂ in the optimized mutant demonstrated the enantioselective cyclopropanation of styrene as well as the mutant containing native heme. Interestingly, rMb*(FePor(CF₃)₂) proceeds the C–H bond insertion of 1-methoxy-4-(methoxymethyl)benzene with a TON value of 2 (Table S8), whereas nMb and rMb(FePc) did not give the desired product. Thus, this strategy has the potential to improve other carbene transfer reactions. Although the redox potentials of hemoproteins can be controlled by modification of the heme pocket through mutagenesis-based protein engineering,^[15] the approach using replacement of the native cofactor with artificial metal porphyrinoid cofactors should provide a more potent and drastic redox shift. Since the different ligand was used in this study, other factors such as the binding mode and affinity of the reactants may also be influential. Therefore, the detailed quantitative contribution of the redox potentials in the cyclopropanation reaction will be clarified using computational simulations in the future. This concept of redox tuning and cofactor engineering of hemoproteins is expected to contribute to development and refinement of important catalytic reactions.

Supporting Information

The authors have cited additional references within the Supporting Information.^[73–83]

Acknowledgements

This work was funded by Grants-in-Aid for Scientific Research provided by JSPS KAKENHI Grant Numbers JP15H05804, JP18KK0156, JP20H02755, JP20H00403, JP20KK0315, JP22H05364, JP22K21348, JP23H03832, JP23K17932 and JST PRESTO JPMJPR15S2 and JPMJPR22A3. Y.K. appreciates the support from the JSPS Research Fellowship for Young Scientists (JSPS KAKENHI Grant Number JP21J20563). K.O. thanks the financial supports by the Tokuyama Science Foundation, the Takeda Science Foundation, and the Noguchi Institute.



Scheme 2. Plausible mechanism for catalytic cyclopropanation by rMb*(FePor(CF₃)₂).

Conflict of Interest

The authors declare no conflict of interest.

Data Availability Statement

The data that support the findings of this study are available from the corresponding author upon reasonable request.

Keywords: reconstituted myoglobin · artificial metalloenzymes · carbenes · alkenes · cyclopropanation

- [1] S. Bähr, S. Brinkmann-Chen, M. Garcia-Borràs, J. M. Roberts, D. E. Katsoulis, K. N. Houk, F. H. Arnold, *Angew. Chem. Int. Ed.* **2020**, *59*, 15507–15511.
- [2] S. C. Hammer, G. Kubik, E. Watkins, S. Huang, H. Minges, F. H. Arnold, *Science* **2017**, *358*, 215–218.
- [3] X. Liu, Y. Yu, C. Hu, W. Zhang, Y. Lu, J. Wang, *Angew. Chem. Int. Ed.* **2012**, *51*, 4312–4316.
- [4] E. N. Mirts, I. D. Petrik, P. Hosseinzadeh, M. J. Nilges, Y. Lu, *Science* **2018**, *361*, 1098–1101.
- [5] A. Bhagi-Damodaran, I. D. Petrik, N. M. Marshall, H. Robinson, Y. Lu, *J. Am. Chem. Soc.* **2014**, *136*, 11882–11885.
- [6] N. Yeung, Y.-W. Lin, Y.-G. Gao, X. Zhao, B. S. Russell, L. Lei, K. D. Miner, H. Robinson, Y. Lu, *Nature* **2009**, *462*, 1079–1082.
- [7] P. S. Coelho, E. M. Brustad, A. Kannan, F. H. Arnold, *Science* **2013**, *339*, 307–310.
- [8] M. Bordeaux, V. Tyagi, R. Fasan, *Angew. Chem. Int. Ed.* **2015**, *54*, 1744–1748.
- [9] V. Tyagi, G. Sreenilayam, P. Bajaj, A. Tinoco, R. Fasan, *Angew. Chem. Int. Ed.* **2016**, *55*, 13562–13566.
- [10] Z. J. Wang, N. E. Peck, H. Renata, F. H. Arnold, *Chem. Sci.* **2013**, *5*, 598–601.
- [11] S. B. J. Kan, R. D. Lewis, K. Chen, F. H. Arnold, *Science* **2016**, *354*, 1048–1051.
- [12] S. B. J. Kan, X. Huang, Y. Gumulya, K. Chen, F. H. Arnold, *Nature* **2017**, *552*, 132–136.
- [13] V. Tyagi, R. B. Bonn, R. Fasan, *Chem. Sci.* **2015**, *6*, 2488–2494.
- [14] V. Tyagi, R. Fasan, *Angew. Chem. Int. Ed.* **2016**, *55*, 2512–2516.
- [15] M. Pott, M. Tinzl, T. Hayashi, Y. Ota, D. Dunkelmann, P. R. E. Mittl, D. Hilvert, *Angew. Chem. Int. Ed.* **2021**, *60*, 15063–15068.
- [16] T. Hayashi, M. Tinzl, T. Mori, U. Krengel, J. Proppe, J. Soetbeer, D. Klose, G. Jeschke, M. Reiher, D. Hilvert, *Nat. Catal.* **2018**, *1*, 578–584.
- [17] R. K. Zhang, K. Chen, X. Huang, L. Wohlschlagel, H. Renata, F. H. Arnold, *Nature* **2019**, *565*, 67–72.
- [18] C. K. Prier, R. K. Zhang, A. R. Buller, S. Brinkmann-Chen, F. H. Arnold, *Nat. Chem.* **2017**, *9*, 629–634.
- [19] S. V. Athavale, S. Gao, A. Das, S. C. Mallojjala, E. Alfonzo, Y. Long, J. S. Hirschi, F. H. Arnold, *J. Am. Chem. Soc.* **2022**, *144*, 19097–19105.
- [20] J. A. McIntosh, P. S. Coelho, C. C. Farwell, Z. J. Wang, J. C. Lewis, T. R. Brown, F. H. Arnold, *Angew. Chem. Int. Ed.* **2013**, *52*, 9309–9312.
- [21] Q. Zhou, M. Chin, Y. Fu, P. Liu, Y. Yang, *Science* **2021**, *374*, 1612–1616.
- [22] W. Fu, N. M. Neris, Y. Fu, Y. Zhao, B. Krohn-Hansen, P. Liu, Y. Yang, *Nat. Catal.* **2023**, *6*, 628–636.
- [23] L. Villarino, K. E. Splan, E. Reddem, L. Alonso-Cotchico, C. Gutiérrez de Souza, A. Lledós, J.-D. Maréchal, A.-M. W. H. Thunnissen, G. Roelfes, *Angew. Chem. Int. Ed.* **2018**, *57*, 7785–7789.
- [24] R. Stenner, J. W. Steventon, A. Seddon, J. L. R. Anderson, *Proc. Natl. Acad. Sci. USA* **2020**, *117*, 1419–1428.
- [25] E. Sansiaume-Dagousset, A. Urvoas, K. Chelly, W. Ghattas, J.-D. Maréchal, J.-P. Mahy, R. Ricoux, *Dalton Trans.* **2014**, *43*, 8344–8354.
- [26] I. Kalvet, M. Ortmayer, J. Zhao, R. Crawshaw, N. M. Ennist, C. Levy, A. Roy, A. P. Green, D. Baker, *J. Am. Chem. Soc.* **2023**, *145*, 14307–14315.
- [27] R. Ricoux, H. Sauriat-Dorizon, E. Girgenti, D. Blanchard, J.-P. Mahy, *J. Immunol. Methods* **2002**, *269*, 39–57.
- [28] R. Ricoux, M. Allard, R. Dubuc, C. Dupont, J.-D. Maréchal, J.-P. Mahy, *Org. Biomol. Chem.* **2009**, *7*, 3208–3211.
- [29] F. Natri, L. Lista, P. Ringhieri, R. Vitale, M. Faiella, C. Andreozzi, P. Travascio, O. Maglio, A. Lombardi, V. Pavone, *Chem. Eur. J.* **2011**, *17*, 4444–4453.
- [30] P. Dydio, H. M. Key, A. Nazarenko, J. Y.-E. Rha, V. Seyedkazemi, D. S. Clark, J. F. Hartwig, *Science* **2016**, *354*, 102–106.
- [31] P. Dydio, H. M. Key, H. Hayashi, D. S. Clark, J. F. Hartwig, *J. Am. Chem. Soc.* **2017**, *139*, 1750–1753.
- [32] H. M. Key, P. Dydio, Z. Liu, J. Y.-E. Rha, A. Nazarenko, V. Seyedkazemi, D. S. Clark, J. F. Hartwig, *ACS Cent. Sci.* **2017**, *3*, 302–308.
- [33] G. Sreenilayam, E. J. Moore, V. Steck, R. Fasan, *Adv. Synth. Catal.* **2017**, *359*, 2076–2089.
- [34] E. J. Moore, V. Steck, P. Bajaj, R. Fasan, *J. Org. Chem.* **2018**, *83*, 7480–7490.
- [35] M. W. Wolf, D. A. Vargas, N. Lehnert, *Inorg. Chem.* **2017**, *56*, 5623–5635.
- [36] T. Hayashi, H. Dejima, T. Matsuo, H. Sato, D. Murata, Y. Hisaeda, *J. Am. Chem. Soc.* **2002**, *124*, 11226–11227.
- [37] T. Hayashi, D. Murata, M. Makino, H. Sugimoto, T. Matsuo, H. Sato, Y. Shiro, Y. Hisaeda, *Inorg. Chem.* **2006**, *45*, 10530–10536.
- [38] T. Matsuo, D. Murata, Y. Hisaeda, H. Hori, T. Hayashi, *J. Am. Chem. Soc.* **2007**, *129*, 12906–12907.
- [39] K. Oohora, Y. Kihira, E. Mizohata, T. Inoue, T. Hayashi, *J. Am. Chem. Soc.* **2013**, *135*, 17282–17285.
- [40] K. Oohora, H. Meichin, Y. Kihira, H. Sugimoto, Y. Shiro, T. Hayashi, *J. Am. Chem. Soc.* **2017**, *139*, 18460–18463.
- [41] K. Oohora, H. Meichin, L. Zhao, M. W. Wolf, A. Nakayama, J. Hasegawa, N. Lehnert, T. Hayashi, *J. Am. Chem. Soc.* **2017**, *139*, 17265–17268.
- [42] K. Oohora, Y. Miyazaki, T. Hayashi, *Angew. Chem. Int. Ed.* **2019**, *58*, 13813–13817.
- [43] Y. Morita, K. Oohora, A. Sawada, K. Doitomi, J. Ohbayashi, T. Kamachi, K. Yoshizawa, Y. Hisaeda, T. Hayashi, *Dalton Trans.* **2016**, *45*, 3277–3284.
- [44] G. Sreenilayam, E. J. Moore, V. Steck, R. Fasan, *ACS Catal.* **2017**, *7*, 7629–7633.
- [45] D. M. Carminati, R. Fasan, *ACS Catal.* **2019**, *9*, 9683–9697.
- [46] D. M. Carminati, J. Decaens, S. Couve-Bonnaire, P. Jubault, R. Fasan, *Angew. Chem. Int. Ed.* **2021**, *60*, 7072–7076.
- [47] O. F. Brandenburg, C. K. Prier, K. Chen, A. M. Knight, Z. Wu, F. H. Arnold, *ACS Catal.* **2018**, *8*, 2629–2634.
- [48] Z. J. Wang, H. Renata, N. E. Peck, C. C. Farwell, P. S. Coelho, F. H. Arnold, *Angew. Chem. Int. Ed.* **2014**, *53*, 6810–6813.
- [49] B. J. Wittmann, A. M. Knight, J. L. Hofstra, S. E. Reisman, S. B. Jennifer Kan, F. H. Arnold, *ACS Catal.* **2020**, *10*, 7112–7116.
- [50] D. Nam, V. Steck, R. J. Potenzino, R. Fasan, *J. Am. Chem. Soc.* **2021**, *143*, 2221–2231.
- [51] A. Tinoco, V. Steck, V. Tyagi, R. Fasan, *J. Am. Chem. Soc.* **2017**, *139*, 5293–5296.

- [52] P. Bajaj, G. Sreenilayam, V. Tyagi, R. Fasan, *Angew. Chem. Int. Ed.* **2016**, *55*, 16110–16114.
- [53] P. S. Coelho, Z. J. Wang, M. E. Ener, S. A. Baril, A. Kannan, F. H. Arnold, E. M. Brustad, *Nat. Chem. Biol.* **2013**, *9*, 485–487.
- [54] A. M. Knight, S. B. J. Kan, R. D. Lewis, O. F. Brandenburg, K. Chen, F. H. Arnold, *ACS Cent. Sci.* **2018**, *4*, 372–377.
- [55] T. Kim, A. M. Kassim, A. Botejue, C. Zhang, J. Forte, D. Rozzell, M. A. Huffman, P. N. Devine, J. A. McIntosh, *ChemBioChem* **2019**, *20*, 1129–1132.
- [56] Y. Wei, A. Tinoco, V. Steck, R. Fasan, Y. Zhang, *J. Am. Chem. Soc.* **2018**, *140*, 1649–1662.
- [57] M. G. Siriboe, D. A. Vargas, R. Fasan, *J. Org. Chem.* **2023**, *88*, 7630–7640.
- [58] H. Toi, M. Homma, A. Suzuki, H. Ogoshi, *J. Chem. Soc. Chem. Commun.* **1985**, 1791–1792.
- [59] N. Ono, H. Kawamura, K. Maruyama, *Bull. Chem. Soc. Jpn.* **1989**, *62*, 3386–3388.
- [60] T. Shibata, S. Nagao, M. Fukaya, H. Tai, S. Nagatomo, K. Morishashi, T. Matsuo, S. Hirota, A. Suzuki, K. Imai, Y. Yamamoto, *J. Am. Chem. Soc.* **2010**, *132*, 6091–6098.
- [61] J. F. Taylor, V. E. Morgan, *J. Biol. Chem.* **1942**, *144*, 15–20.
- [62] J. R. Wolf, C. G. Hamaker, J.-P. Djukic, T. Kodadek, L. K. Woo, *J. Am. Chem. Soc.* **1995**, *117*, 9194–9199.
- [63] H. M. Key, P. Dydio, D. S. Clark, J. F. Hartwig, *Nature* **2016**, *534*, 534–537.
- [64] T. Shibata, D. Matsumoto, R. Nishimura, H. Tai, A. Matsuoka, S. Nagao, T. Matsuo, S. Hirota, K. Imai, S. Neya, A. Suzuki, Y. Yamamoto, *Inorg. Chem.* **2012**, *51*, 11955–11960.
- [65] B. A. Springer, S. G. Sligar, J. S. Olson, G. N. Jr Phillips, *Chem. Rev.* **1994**, *94*, 699–714.
- [66] X. Jiang, G. Ji, *J. Org. Chem.* **1992**, *57*, 6051–6056.
- [67] X. Jiang, *Acc. Chem. Res.* **1997**, *30*, 283–289.
- [68] H. J. Callot, T. Tschamber, *J. Am. Chem. Soc.* **1975**, *97*, 6175–6178.
- [69] L. Latos-Grazynski, R.-J. Cheng, G. N. La Mar, A. L. Balch, *J. Am. Chem. Soc.* **1981**, *103*, 4270–4272.
- [70] In this study, a porphycene ligand, which has different structural factor than a porphyrin ligand, was employed. This is caused by the limited redox potential range of porphyrin derivatives bound into the protein matrix. The influence of the ligand structure on the binding mode and binding affinity of reactants with the iron center can be considered as an artifact. Although the details should be evaluated, this work focuses on discussing only the differences in experimentally available redox potentials.
- [71] J. Zhang, A. O. Maggiolo, E. Alfonzo, R. Mao, N. J. Porter, N. M. Abney, F. H. Arnold, *Nat. Catal.* **2023**, *6*, 152–160.
- [72] J. Zhang, X. Huang, R. K. Zhang, F. H. Arnold, *J. Am. Chem. Soc.* **2019**, *141*, 9798–9802.
- [73] X. Ren, B. M. Couture, N. Liu, M. S. Lall, J. T. Kohrt, R. Fasan, *J. Am. Chem. Soc.* **2023**, *145*, 537–550.
- [74] F. W. J. Teale, *Biochim. Biophys. Acta* **1959**, *35*, 543.
- [75] K. S. Feldman, R. E. Simpson, *J. Am. Chem. Soc.* **1989**, *111*, 4878–4886.
- [76] K. Kamata, T. Kimura, N. Mizuno, *Chem. Lett.* **2010**, *39*, 702–703.
- [77] P. Emsley, B. Lohkamp, W. G. Scott, K. Cowtan, *Acta Crystallogr. Sect. D* **2010**, *66*, 486–501.
- [78] W. Kabsch, *Acta Crystallogr. Sect. D* **2010**, *66*, 133–144.
- [79] K. Yamashita, K. Hirata, M. Yamamoto, *Acta Crystallogr. Sect. D* **2018**, *74*, 441–449.
- [80] A. Vagin, A. Teplyakov, *J. Appl. Crystallogr.* **1997**, *30*, 1022–1025.
- [81] M. D. Winn, C. C. Ballard, K. D. Cowtan, E. J. Dodson, P. Emsley, P. R. Evans, R. M. Keegan, E. B. Krissinel, A. G. W. Leslie, A. McCoy, S. J. McNicholas, G. N. Murshudov, N. S. Pannu, E. A. Potterton, H. R. Powell, R. J. Read, A. Vagin, K. S. Wilson, *Acta Crystallogr. Sect. D* **2011**, *67*, 235–242.
- [82] G. N. Murshudov, A. A. Vagin, E. J. Dodson, *Acta Crystallogr. Sect. D* **1997**, *53*, 240–255.
- [83] W. Kabsch, *Acta Crystallogr. Sect. D* **2010**, *66*, 125–132.
- [84] K. Hirata, K. Yamashita, G. Ueno, Y. Kawano, K. Hasegawa, T. Kumasaka, M. Yamamoto, *Acta Crystallogr. Sect. D* **2019**, *75*, 138–150.

Manuscript received: February 19, 2024

Accepted manuscript online: May 23, 2024

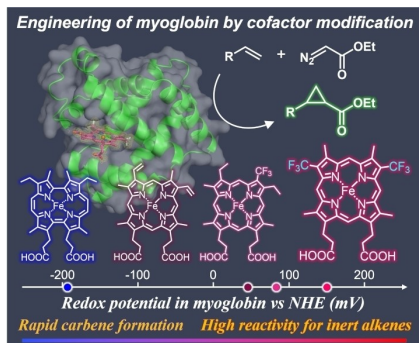
Version of record online: ■■■, ■■■

Research Article

Artificial Metalloenzymes

Y. Kagawa, K. Oohora,* T. Himiyama,
A. Suzuki, T. Hayashi* — e202403485

Redox Engineering of Myoglobin by Cofactor Substitution to Enhance Cyclopropanation Reactivity



Redox-diverse myoglobins containing four different cofactors with different redox potentials (−198 to +147 mV vs. NHE) were studied as catalysts for alkene cyclopropanation through carbene transfer. Myoglobin with a positive redox potential is highly reactive for electron-deficient alkenes, such as 1-octene. In contrast, myoglobin with a negative redox potential accelerates the formation of a detectable carbene intermediate.